Published in Applied Optics, 50, 19, G20-G25 (1 July 2017)

Iridescent clouds and distorted coronas

PHILIP LAVEN

9 Russells Crescent, Horley, RH6 7DJ, United Kingdom philip@philiplaven.com

Received 16 February 2017; accepted 20 March 2017; posted 4 April 2017 (Doc. ID 286878); published 26 April 2017

Near-forward scattering of sunlight generates coronas and iridescence on clouds. Coronas are caused by diffraction, whereas iridescence is less easily explained. Iridescence often appears as bands of color aligned with the edges of clouds or as apparently random patches of color on clouds. This paper suggests that iridescence is due to interference between light that has been diffracted by a spherical droplet of water and light that has been transmitted through the same droplet.

OCIS codes: (010.1290) Atmospheric optics *(290.1310); Atmospheric scattering; (290.2558) Forward scattering.*

https://doi.org/10.1364/AO.56.000G20

1. INTRODUCTION

Iridescent clouds are unlike other atmospheric phenomena, such as coronas, rainbows and glories, in that they do not appear as colored circular arcs. The iridescence typically appears in the form of bands of color following the edges of clouds or irregular patches of color on clouds.

The principal aim of this paper is to offer an explanation for the scattering mechanisms that result in iridescent clouds.

Section 2 shows that some types of iridescence are actually distorted coronas, whilst section 3 examines various images of iridescence on clouds. Section 4 uses Mie theory to identify conditions that could generate iridescence. Section 5 offers some conclusions.

2. THE CORONA

The corona and iridescent clouds are both caused by near-forward scattering, but the two phenomena are subtly different. The idealized corona, as illustrated in Fig. 1, appears as a series of concentric colored rings centered on the sun or moon with a predictable sequence of colors.

Simulations of the scattering of sunlight [1] show that droplet radius r can be determined from the angular radii of the three inner red rings of the corona using the relationships $r \approx 16/\theta_1$, $r \approx 31/\theta_2$ and $r \approx 47/\theta_3$, when θ is measured in degrees and r is measured in μm. In the case of Fig. 1, the rings correspond to scattering by droplets of radius $r \approx 4.8$ μm.

In practice, there is not always a clear distinction between coronas and iridescent clouds – as illustrated by the two images in Fig. 2. The image in Fig. 2(a) shows a corona with broad colored rings, whilst Fig. 2(b), which was taken about 4 minutes later than Fig. 2(a), shows that the rings of the corona have become colored bands that are no longer concave towards the sun.

Pictures of the corona, including those in Fig. 2, are usually framed to avoid the sun, thus allowing the camera to capture the delicate details of the corona's rings. Unfortunately, this tactic makes it more difficult to estimate the position of the sun in the images. Nevertheless, Fig. 3 shows the images with circles centered on the assumed position of the sun, thus allowing the scattering angle θ to be determined for various features of the corona. Fig. 3 also shows the estimated radius of droplets generating the second red ring of the corona, using the relationship $r = 31/\theta_2$. Fig. 3(a) confirms that the second red ring is not quite circular: this distortion is due to slight variations of r across the cloud. Fig. 3(b) shows larger variations in r, resulting in the rings being transformed into almost straight bands of color.

Fig. 4 shows yet another distorted corona: in this case, the distortion of the rings is very symmetrical. A similar corona was shown in [2] where it was described as "an asymptotic corona". Fig. 5 shows a simulation based on a linear decrease in r from 10 μm to 1 μm. Although this size profile is completely arbitrary, the resulting simulation is remarkably similar to the distorted corona shown in Fig. 4 – thus providing indirect confirmation that the distortion is due variations in the size of cloud droplets.

Fig. 1 Multi-ringed lunar corona © Lauri Kangas

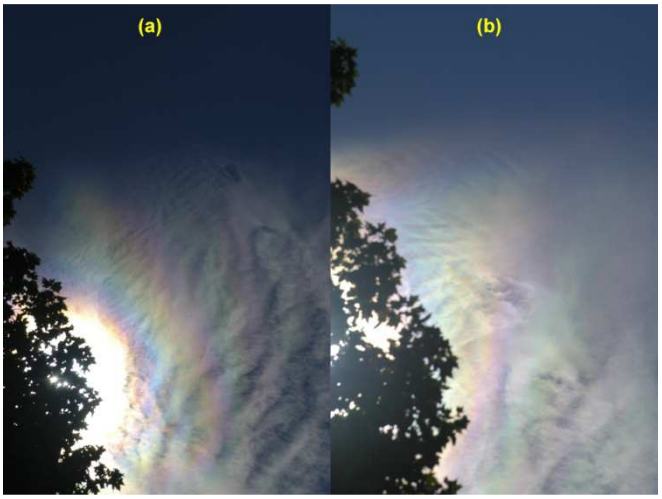

Fig. 2 A corona or iridescence? Image (a) looks like a corona because the colored rings are roughly circular and centered on the sun. Image (b), taken 4 minutes later, shows that the rings have been transformed into iridescent bands of color. © Lauri Kangas

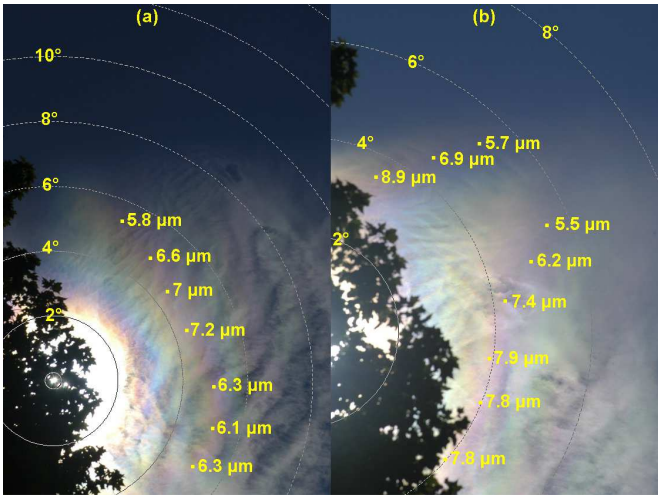

Fig. 3 As Fig. 2 but showing circles around the sun at intervals of 2°, together with estimates of the radius of droplets forming the second red ring of the corona. © Lauri Kangas.

Fig. 4 A symmetrically-distorted corona. © August Allen.

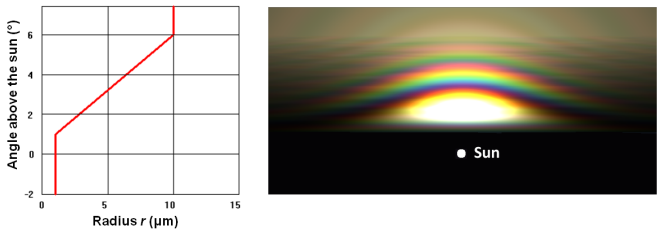

Fig. 5 Mie theory simulation assuming that the cloud droplets have the size profile shown in the graph on the left.

3. FEATURES OF IRIDESCENT CLOUDS

The previous section implies that many observations of distorted coronas are wrongly classified as iridescence: this is understandable because there is no straightforward definition of "iridescence". Some suggest that it means "luminous colors that change with viewing angles" as with the beautiful feathers of some birds, whilst others use it simply to mean "rainbow-like" colors.

On the basis that "a picture is worth a thousand words", it is more productive to examine some images of iridescent clouds. For example, there is no doubt that the stunning image in Fig. 6 shows iridescence. Some of the colors on the cloud at the top center of the image are saturated, but the other clouds show more delicate variations in color. The sharply-curved bands of color are especially striking. At first sight, they seem similar to the rings of a corona – but that would require the sun to be in the center of the large cloud. There are no obvious clues in Fig. 6 that would unambiguously identify the relative position of the sun.

Fig. 7 shows an extract from another image taken at about the same time as Fig. 6. Fortuitously, various faint shadows at the top right of Fig. 7 indicate the direction of the sun. Based on this information, circles at intervals of 2° centered on the sun have been added to Fig. 7. These indicate that the iridescence on the clouds was at its brightest for scattering angles θ between 5° and 8°, with some weaker iridescence appearing when $\theta < 12°$.

Fig. 8 shows another magnificent image of colored bands along the edges of clouds. In this case, we have no information about the relative position of the sun – apart from the fact that the photographer (Pat Gaines) deliberately used a 500 mm telephoto lens to capture the details of the cloud whilst avoiding the glare of the sun, suggesting that $\theta < 10°$.

Figs. 9 and 10 show clouds with numerous patches of color. Both images include some colored bands aligned with the edges of the clouds, but it is difficult to see any pattern in these patches of fairly uniform color. This apparently random arrangement of colors is fairly typical of iridescent clouds – even appearing as far away as $\theta = 35°$.

Fig. 6 Iridescent clouds over Mt. Thamserku (6604 m) the Himalayas on 18 October 2009 showing bands of color along the edges of clouds. © Oleg Bartunov.

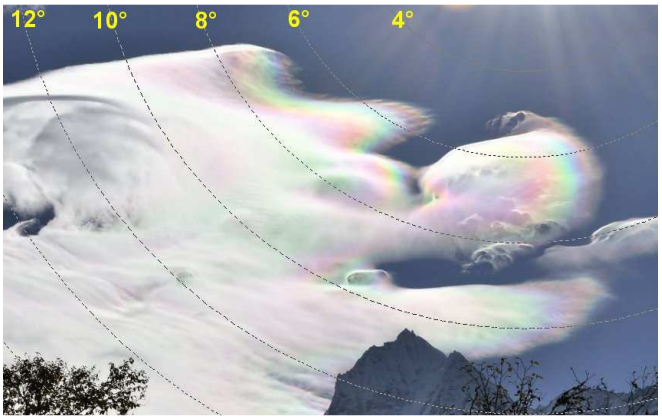

Fig. 7 A similar image (taken 1 minute before Fig. 6) showing shadows indicating the direction of the sun. The circles shows the angular separation from the sun at intervals of 2°. © Oleg Bartunov.

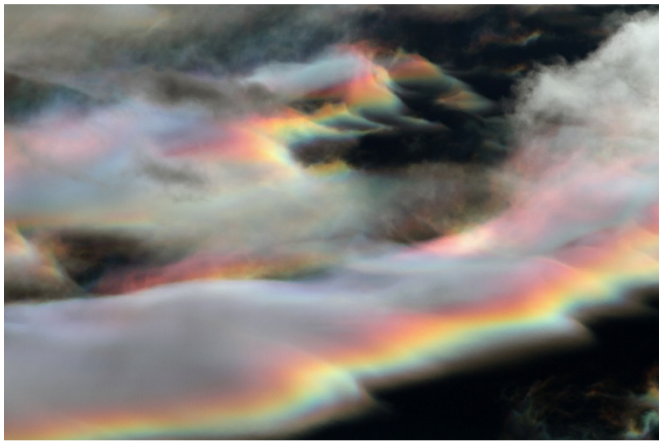

Fig. 8 Bands of color along the edges of clouds as seen in Colorado. © Pat Gaines

Fig. 9 Iridescent clouds showing patches of color.

Fig. 10 An iridescent cloud showing patches of color. © Emil Ivanov.

4. SCATTERING MECHANISMS

The corona can be modeled using diffraction theory, as summarized in Fig. 11. As noted in [1], the three inner red rings of the corona occur at $\theta = 16/r$, $33/r$ and $47/r$, where the scattering angle θ is measured in degrees and the droplet radius r is measured in μm. As the axes of Fig. 11 use logarithmic scales, the lines corresponding to a specific color are straight lines. The absolute intensity of scattered light varies dramatically across the range of angles and droplet sizes shown in Fig. 11. It is therefore impossible for this image to reproduce the full dynamic range of the scattered light. Hence, this and subsequent diagrams display only the saturated colors of the scattered light.

Fig. 12 shows an equivalent diagram which has been calculated using Mie theory. Comparing Figs. 11 and 12, diffraction theory and Mie theory give fairly similar results for $r > 5$ μm, but there are dramatic differences elsewhere. [1, 3, 4] For example, the Mie results for 0.5 μm < r < 3 μm and $\theta < 10°$ consist of colors that vary with r but are almost independent of θ. Furthermore, very complicated patterns of color appear at $\theta > 10°$.

What causes the extraordinary patterns in Fig. 12? Fig. 13 shows another diagram which shows the combined contributions of the Debye series $p = 0$ and $p = 1$ terms. The $p = 0$ term corresponds to diffraction and external reflection from the droplet, whilst the $p = 1$ term corresponds to light that has been transmitted through the droplet. The close agreement between Figs. 12 and 13 indicates that most of strange patterns are the result of interference between diffracted and transmitted light. The term "anomalous diffraction" was adopted by van de Hulst [5] to denote the resulting differences between diffraction theory and Mie theory.

One feature missing from Figs. 11 and 13 is the blue color appearing in Fig. 12 as $r \rightarrow 0.1$ μm: this indicates the transition towards Rayleigh scattering.

Fig. 12 demonstrates that diffraction theory should be used with great care for calculations of scattering from water droplets with $r < 5$ μm. Perhaps, more importantly, we need to examine whether the complicated patterns shown in Fig. 12 have any observable consequences in nature. The vertical colored lines at the top of Fig. 12, which are shown in more detail in Fig. 14, indicate that sunlight scattered at $\theta < 10°$ by water droplets with $r = 1.6$ μm would appear to be red, whilst sunlight scattered by water droplets with $r = 1$ μm would appear to be blue.

Some cloud types, such as lenticular clouds, are well-ordered in terms of droplet size. [6, 7] The edges of a lenticular cloud (i.e. the lowest layer) have the smallest droplets, whereas the tops of such clouds have the largest droplets – with a gradual change in drop size between these two extremes. As the scattering patterns in Fig. 14 are approximately independent of θ when $\theta < 10°$, we might expect lenticular clouds to display some form of iridescence. For example, the colors appearing on the lenticular clouds in Fig. 8 could indicate the presence of very small water droplets. To be specific, the dominant red bands could be caused by droplets with $r \approx 1.6$ μm. Similarly, just below the red bands, there is a narrow band of yellow ($r \approx 1.45$ μm), followed by a band of cyan ($r \approx 1.15$ μm). At the bottom edge of the cloud, there is another faint band of red, which could be due to droplets with $r \approx 0.9$ μm. Note that the clouds in Fig. 8 do not display any other colors above the dominant red band, which is consistent with the results shown in Fig 12 for droplets with $r > 2$ μm.

Fig. 15 is an enlarged section of Fig. 12 showing the complicated patterns that occur when 1 μm < r < 3 μm and $\theta > 10°$. Careful examination of Fig, 15 reveals that patches of fairly uniform color are separated by very narrow bands of yellow or cyan. Do these patches of color, defined by r and θ, result in any observable patterns in nature? If r is constant across a cloud, the scattered color will vary as a function of θ – as in the simulations for $r = 1.5$ μm in Fig. 16(a) and (b) which show corona-like circular colors. Much more complicated patterns can appear if r is not constant – as shown in Fig. 16(c) and (d) which assume that r varies from 2 μm at the top of the image to 1 μm at the bottom of the image. As gradual variations of droplet size frequently occur in clouds, such scattering could be responsible for the colored patches could appear on individual clouds. However, as the value of θ changes when clouds move, it is likely that the precise nature of these colored patches will change quite quickly. Observations of iridescence patches on clouds confirm that they are typically very short-lived.

These explanations are applicable to clouds composed of liquid water droplets, but many clouds could be too cold for water droplets to be in liquid form. For example, it is not clear whether the clouds shown in Figs. 6 and 7 contain liquid water. Nevertheless, it is suggested that bands of color aligned with the edges of clouds at $\theta < 10°$ are a strong indicator of the presence of spherical droplets of water with 0.5 μm < r < 3 μm.

Polar stratospheric clouds, as shown in Fig. 17, also exhibit bands of color along their edges. Such clouds may not contain water droplets, but they probably contain various other substances, such as nitric acid or sulfuric acid. Fig. 18 shows the results of Mie theory calculations for scattering by spherical droplets of sulfuric acid. This diagram is similar to Fig. 12 except that the vertical bands of color occur at slightly smaller values of r (e.g. red bands at $r \approx 1.2$ μm and $r \approx 0.7$ μm, compared with $r \approx 1.6$ μm and $r \approx 0.9$ μm for water). Fig. 18 also shows that scattering by droplets of sulfuric acid of 0.4 μm < r < 1.5 μm is almost independent of θ when $\theta < 15°$, compared with $\theta < 10°$ for water. Is it possible that Mie theory can also explain the colored bands on polar stratospheric clouds?

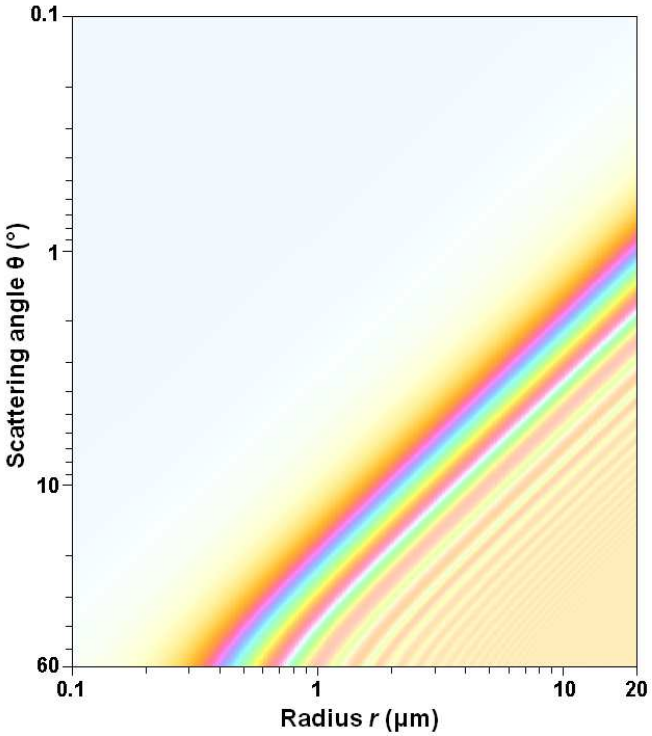

Fig. 11 A diagram calculated using diffraction theory showing how the saturated colors of the corona vary with scattering angle θ and radius r of a spherical droplet of water.

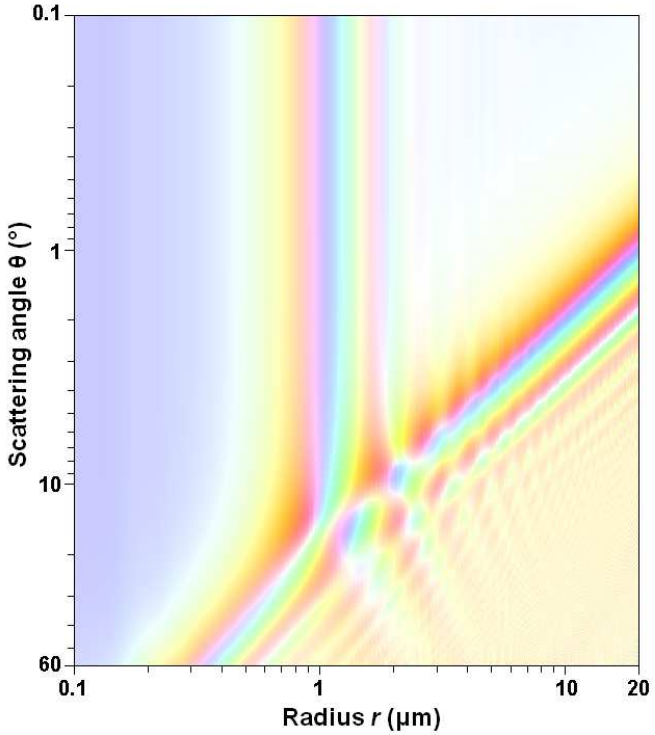

Fig. 12 As Fig. 11 but calculated using Mie theory.

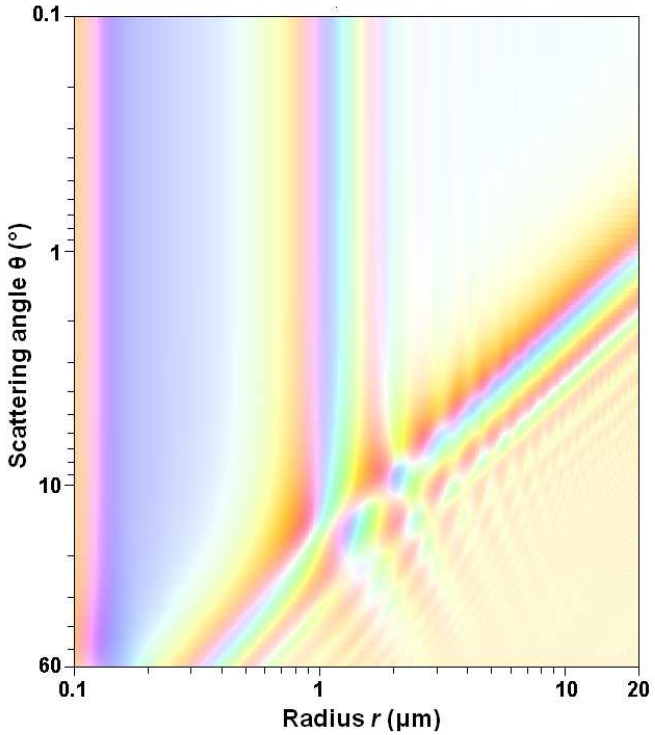

Fig. 13 As Fig. 10, but showing the combined effects of the $p = 0$ and $p = 1$ terms of the Debye series.

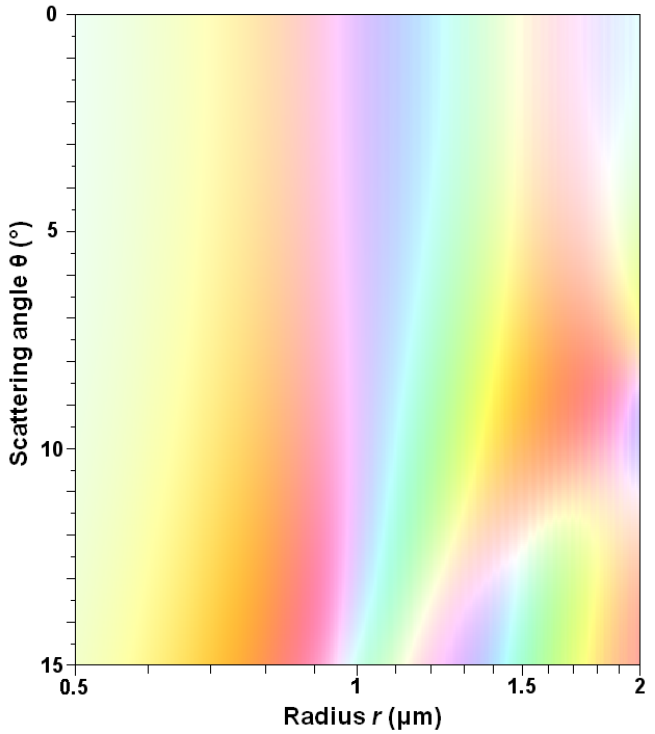

Fig. 14 Enlarged section of Fig. 12 showing that the scattered colors are almost independent of scattering angle θ.

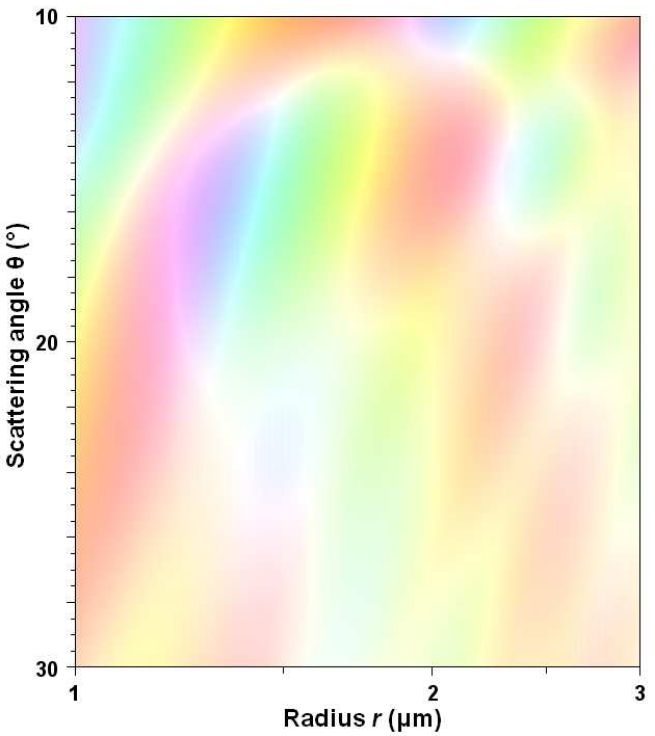

Fig. 15 Enlarged section of Fig. 12 showing blocks of colors dependent on the values of r and θ.

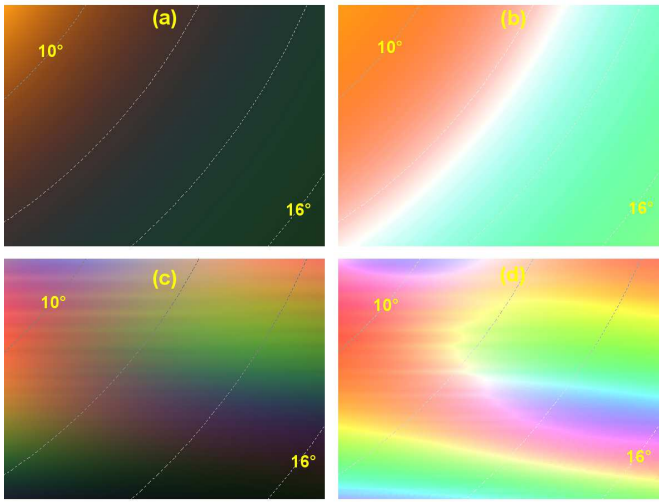

Fig. 16 Simulations of scattering of sunlight by water droplets. (a) and (b) show results for r = 1.5 µm, whilst (c) and (d) assume that the droplet size r varies linearly from r = 2 µm at the top of the image to r = 1 µm at the bottom of the image. The simulations show the natural colors in (a) and (c) and saturated colors in (b) and (d).

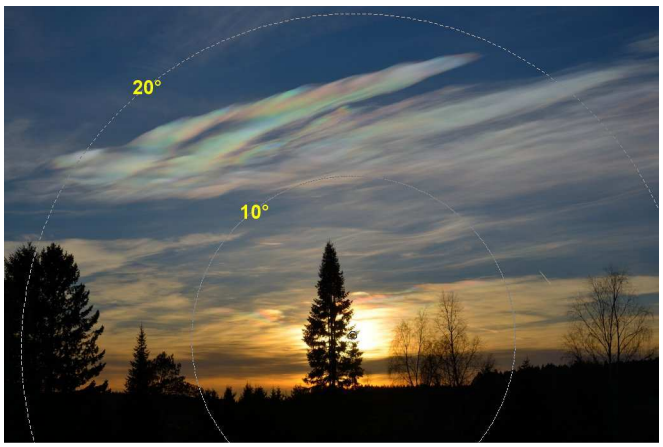

Fig. 17 Polar stratospheric clouds observed in Finland © Matti Helin.

5. CONCLUSIONS

Coronas are caused by diffraction by cloud droplets. If the droplets are uniform in size, the colored rings of the corona will be circular. If the droplets vary in size across the cloud, the rings of the corona will be distorted. Such behavior can be readily explained using Fraunhofer diffraction theory.

This paper presents the hypothesis that iridescence is due to interference between the light that has been diffracted by a droplet and the light that has been transmitted through that droplet. The Mie theory diagram in Fig. 12 for the scattering of sunlight by spherical water droplets provides a simple explanation for two types of iridescence on clouds:

a) bands of color following the edges of clouds at scattering angles $\theta < 10°$ are caused by droplets of radius 0.5 µm < r < 2 µm (because the scattered color is independent of θ);

b) apparently random patches of pastel colors on clouds when $10° < \theta < 35°$ are caused by gradual variations in droplet sizes in the approximate range 1 µm < r < 3 µm

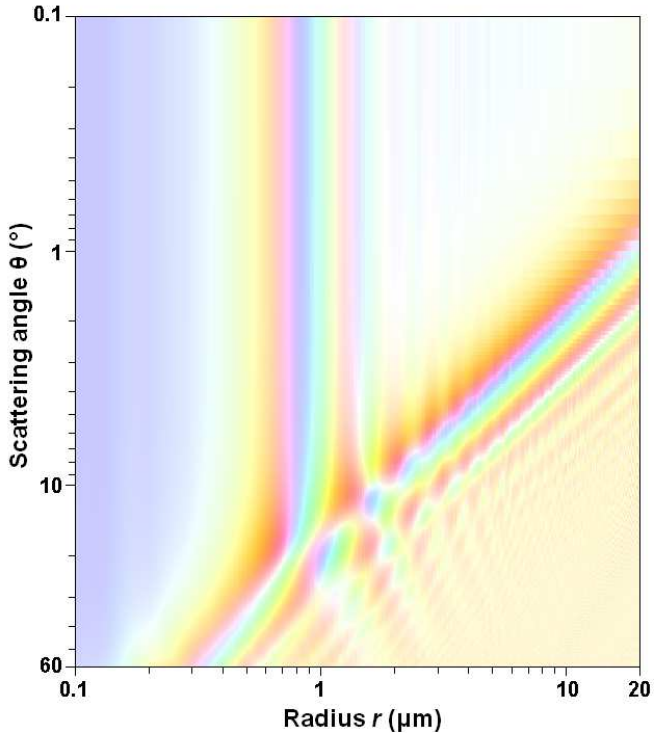

Fig. 18 As Fig. 12 but for droplets of sulfuric acid (H_2SO_4).

ACKNOWLEDGEMENT

The author would like to thank Günther Können for numerous helpful discussions on this topic.

REFERENCES

1. P. Laven, "Re-visiting the atmospheric corona," Appl. Opt. **54**, B46-B53 (2015).
2. J. A. Shaw and P. J. Neiman, "Coronas and iridescence in mountain wave clouds," Appl. Opt. **42**, 476–485 (2003).
3. P. Laven, "Simulation of rainbows, coronas and glories using Mie theory and the Debye series," J. Quant. Spectrosc. Radiat.Transfer **89**, 257–269 (2004).
4. S. D. Gedzelman and J. A. Lock, "Simulating coronas in color," Appl. Opt. **42**, 497–504 (2003).
5. H. C. van de Hulst, *Light Scattering by Small Particles* (Dover, New York, 1981; reprint of 1957 edition).
6. C. D. Whiteman, *Mountain Meteorology: Fundamentals and Applications*, OUP USA (2000).
7. Z. Cui, A. M. Blyth, K. N. Bower, J. Crosier and T. Choularton, "Aircraft measurements of wave clouds," Atmos. Chem. Phys. **12**, 9881-9892 (2012).